

REAL-TIME ELLIPSOMETRY FOR MONITORING THE GROWTH OF CESIUM-TELLURIDE PHOTOCATHODES

P.J.M. van der Slot*, R.A. Loch, M. Tesselaar, M.J.H. Luttkhof,
L. Prodan, J.W.J. Verschuur, K.J. Boller

Laser Physics and Nonlinear Optics, Mesa⁺ Institute for Nanotechnology
University of Twente, PO Box 217, 7500 AE Enschede, The Netherlands

Abstract

Semiconductor photocathodes, especially Cesium-Telluride photocathodes, are vital for generation of high brightness electron beams used in free-electron lasers. However the quantum efficiency and lifetime depends critically on manufacturing and operational conditions. Monitoring the formation of the photocathode is essential for understanding these dependencies. For example, the deposition rate of the Cs correlates to the quantum efficiency and adversely correlates to the lifetime. We will discuss the use of ellipsometry for monitoring the formation of the photocathode, describe our experimental configuration and discuss preliminary results obtained with Cesium-Telluride photocathodes. These results seem to indicate that ellipsometry is a viable method for monitoring the formation of these photocathodes.

INTRODUCTION

Semiconductor photocathodes are used in numerous applications, such as in photodetectors, but also for fundamental research, such as in electron accelerators [1] for free-electron lasers (FELs) and electron-positron colliders. Such cathodes usually consist of a bulk metal substrate with a high melting temperature, coated with a thin semiconductor layer to provide a low work function. A favorite choice for the semiconductor material is Cesium-Telluride (Cs-Te), because it offers the best compromise between a high quantum efficiency (QE) of about 10 % and a long lifetime of several months [2–5]. Due to its high chemical reactivity the Cs-Te layer is deposited in vacuum onto the bulk substrate inside a so-called preparation chamber. The coated cathode can then be used in an accelerator, either directly inserted from the preparation chamber with a vacuum feed-through or transported under ultrahigh vacuum conditions. Because the quantum efficiency drops during cathode operation, a repeated re-fabrication or re-conditioning has to be done and most users of such cathodes prepare their photocathodes at their own location with their specific equipment.

The general belief that Cs-Te is the best choice is weakened by its inconsistent behaviour. This can be seen from reports on the performance of such photocathodes which differ considerably between various groups [2–17]. It was suspected that this lack of reproducibility is related to the

choice of the substrate material [6, 18, 19], its temperature [8], its surface roughness [7, 18], the used thickness of the Cs-Te layer [20], but also to surface contamination by hydrocarbons or oxygen in the preparation or accelerator chamber [12, 18, 21]. Correspondingly, much research has been performed on the influence of such parameters including rejuvenation of photocathodes with cleaning and re-coating [13, 16, 18–21]. Nevertheless, even when restricting to Mo substrates and accounting for the variation of the named parameters, the performance of Cs-Te photocathodes is unpredictable to an extent that is not yet fully understood [18, 21–23].

From comparison of previously published data and own measurements we have postulated that it is mainly the preparation conditions which influences the performance of the photocathodes, while other parameters are less relevant [5]. Specifically, it appears that a layered structure of various different stoichiometric compounds of Cs-Te can form as a result of different Cs deposition rates. As a result, layers with various different ratios of Cs and Te, such as Cs₃Te₂ or Cs₂Te₃ will lead to different surface properties and hence, the variation in observed performance.

The normal procedure of monitoring the QE and deposited mass (using a micro balance) during growths of the photocathode is insufficient to obtain information about its composition. Therefore, another diagnostic is required to test this postulate, and, more important, improve our understanding of the cathode formation process. Ellipsometry may be such a diagnostic, as it is typically used to measure the thickness and composition of thin layers of material [24]. In the remaining sections we briefly discuss the manufacturing of our cathodes, an setup for ellipsometry and preliminary data obtained with the ellipsometry diagnostic.

CATHODE FORMATION

In our experimental setup we use a preparation chamber attached to a 1.3 GHz, 5 $\frac{1}{2}$ cell RF-accelerator. The cathode is mounted on a manipulator arm to transfer the cathode between accelerator and preparation chamber. The cathode consists of a polished Molybdenum (Mo) substrate. First, the cathode is cleaned by heating it to about 600 °C for a few hours. During deposition of the Cs and Te, the cathode is maintained at a temperature of 120 °C to increase the mobility of the atoms deposited. The Te and Cs sources are Mo containers filled with 99.999 % Te pieces and Cs chromate, and are resistively heated. Thermocouples are

* p.j.m.vanderslot@utwente.nl

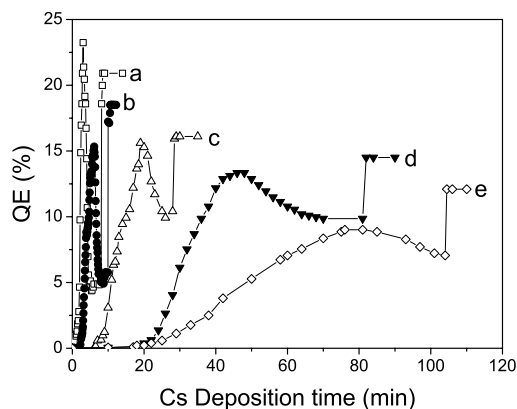


Figure 1: QE (photocurrent), measured at 254 nm, as function of the Cs deposition time for several photocathodes.

used to measure the container's temperature. Typically, the Te and Cs containers are heated to 305 °C and 580 °C respectively. The containers are mounted on a second manipulator arm and one container at a time can be positioned in front of the cathode. The background pressure of the preparation chamber is around 10^{-9} mbar. During the evaporation of Te and Cs we monitor the photocurrent using 254 nm filtered light from a mercury lamp. The available optical power of the filtered light can be varied between 1.4 and 30 μ W. Typically, deposition of Te takes 25 to 30 minutes, and conditions for Cs deposition are varied. We estimate that the Te-layer is about 30 nm thick for 30 minutes deposition time. The containers are moved away from the cathode before cooling them down.

Several examples of the QE (i.e., photocurrent response) are shown in fig. 1 for five different cathodes (a) to (e) made with different Cs deposition rates. Based on the data from ref. [3] we estimate a deposition rate of around 1 nm/min when the maximum QE is obtained after about 80 minutes (cathode (e)). Small oscillations on the curves due to fluctuations in the power of the mercury lamp have been averaged out. Usually, deposition is stopped at the peak in the QE. Here, the Cs deposition has been prolonged after the maximum photocurrent was reached for illustrating purposes. The photocurrent then decreases for all curves and when we removed the Cs source, the current rises immediately. This is due to a combination of partly block UV light by the Cs container (if the final QE is larger than the maximum earlier in the trace) and a quick evaporation of loosely bound, excess Cs from the surface that builds up due to continued Cs deposition after the maximum QE has been obtained [5].

Fig. 1 shows that the maximum QE decreases when the Cs deposition time is increased, i.e., for lower Cs deposition rates. The photocathodes (a,b) that are prepared with a few minutes of Cs deposition have QE's higher than 20%. The photocathode (e), which obtains the maximum photocurrent after 80 minutes, has a QE of 12%, which is

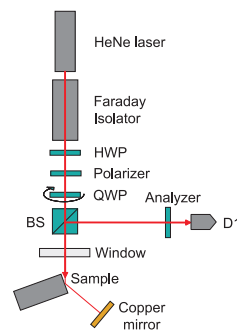


Figure 2: Schematic view of the modified Rotating Compensator Ellipsometer. Everything below the window is internal to the preparation chamber

the same value as reported in ref. [3] for photocathodes prepared with 70 to 80 minutes of Cs deposition. Using a longer Cs deposition time to reach maximum QE, i.e., using a lower Cs deposition rate, usually leads to a more robust photocathode with a longer lifetime. The observed correlation between Cs deposition rate and cathode performance suggests that the various deposition rates leads to a, possibly layered, cathode structure with different Cs-Te ratios [5, 18]. Ellipsometry, as a non-destructive diagnostic, may provide us with additional, real-time information on the structure of the photocathode during its formation.

ELLIPSOMETRY MEASUREMENTS

Ellipsometry is based on preparation of light in a known polarization state and measuring the changes in the polarization state after reflection on the sample surface [24]. In our case the sample consists of a Mo substrate covered with a growing Cs-Te film that may contain various stoichiometries. The Fresnel amplitude reflection coefficients R^p and R^s , for p - and s -polarized incident light respectively, are in general complex and different. Both the amplitude and phase of the reflection coefficients are influenced by the (complex) index of refraction of the film and its thickness. In ellipsometry, two angles are defined, Ψ and Δ , where

$$\tan(\Psi)e^{i\Delta} = R^p/R^s. \quad (1)$$

The information about the film is contained in the ellipsometric variables Ψ and Δ and measuring these values during the growth of the film allows calculation of film thickness and complex index of refraction [24].

Various versions of the ellipsometer exists, each having advantages and disadvantages [24]. Here, we considered the rotating compensator ellipsometer (RCE), see fig. 2. The incident light is produced by a HeNe laser protected by an optical isolator and a halfwave plate is used to control the overall light intensity. The incident polarization is determined by the polarizer and a rotating quarter wave plate that acts as compensator. Because our preparation chamber only has a single usable window, we use a mirror in the

preparation chamber to send the beam back along its path after reflection on the photocathode. The beam therefore reflects twice of the photocathode. After the beam leaves the preparation chamber, a beam splitting cube is used to separate the reflected from the incident beam and direct it to the analyzer and detector (D1). To simplify the analysis, the angles of the polarizer and analyzer are set to 45° . The polarizers used for the polarizer and analyzer are made from nanoparticles in sodium-silicate glass for an increased extinction ratio. By rotating the compensator, the incident light samples all possible polarization states and the detected light intensity I varies with the compensator angle C as [25]

$$I(C) = A_0 + A_2 \cos(2C) + B_2 \sin(2C) + A_4 \cos(4C) + B_4 \sin(4C).$$

The Fourier coefficients A_0 to B_4 are related to the ellipsometric variables Ψ and Δ by [25]

$$\begin{aligned} \Psi &= \arctan\left(\frac{A_2}{2B_4 \sin \Delta}\right) \\ \Delta &= \arctan\left(\frac{A_2}{2A_4}\right) \end{aligned} \quad (2)$$

in case of a single reflection of a sample and without a window present. These equations can be obtained using Mueller matrices for the various optical components to relate the light from the HeNe laser to the light on the detector [24]. The Fourier coefficients still contain the intensity of the HeNe laser, however, as the expressions for the ellipsometric variables (eqs. 2) only contain the ratio of the Fourier coefficients, the dependency on the source light intensity disappears. The only requirement is that the laser power remains constant during a single revolution of the compensator. Similarly, in case of a double reflection on the sample (see fig. 2) eqs. 2 change into

$$\begin{aligned} \Psi &= \frac{1}{2} \arccos\left(-\frac{A_0 + A_4}{2B_4} \pm \sqrt{\left(\frac{A_0 + A_4}{2B_4}\right)^2 - 1}\right) \\ \Delta &= \arctan\left(-2\frac{A_4}{A_2} \pm \sqrt{4\frac{A_4^2}{A_2^2} - 1}\right) \end{aligned} \quad (3)$$

and again, only the ratio of the Fourier coefficients appear in eqs. 3. It should be noted that for the case of no vacuum window, the analysis shows that B_2 should be zero for both a single and double reflection on the sample. It should also be noted that this equation is only illustrative as the vacuum window is not included in the calculation since we do not know the ellipsometric properties of this window. It is therefore not possible to retrieve the ellipsometric angle Ψ and Δ from our measured Fourier coefficients with the current experimental setup. It is planned to install a new, fully characterized window the next time that the preparation chamber will be opened. Nevertheless, by installing the rotating compensator ellipsometer on our preparation

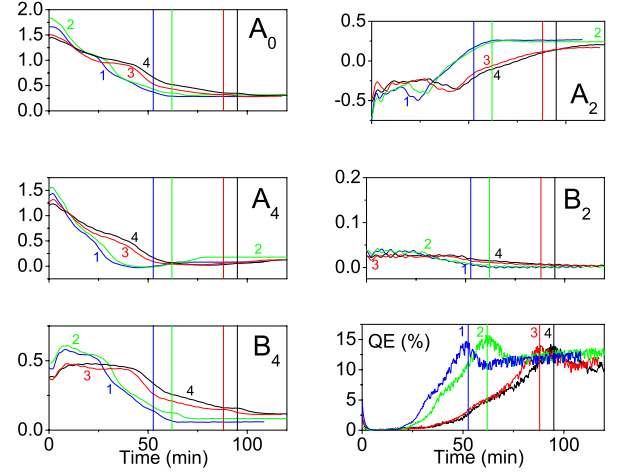


Figure 3: Fourier coefficients A_0 to B_4 and quantum efficiency (QE) as a function of Cs deposition time for various deposition rates of Cs. The vertical lines indicate the position of maximum QE.

chamber we should be able to measure the Fourier coefficients for various Cs deposition rates.

Fig. 3 shows the quantum efficiency (QE) and preliminary Fourier coefficients A_0 to B_4 as a function of the Cs deposition time for four different cathodes (1 to 4) made with different Cs deposition rates. Again the Cs deposition is continued after the maximum QE has been obtained for illustrative purpose. Deposition is continued until the QE reaches a steady state, where the deposited Cs is balanced by evaporation of Cs from the cathode [5]. The maximum QE is 14 % and 15 % for cathodes (1) and (2) respectively, while it is 13 % for the cathodes (3) and (4). The absolute error in the measurement of the QE is of the order $\pm 1\%$. Based on the maximum QE, one would expect the cathodes (3) and (4) to be very similar, as the QE response is the same up to a Cs deposition time of 75 minutes. For later times the QE starts to differ slightly, while the QE in steady state is again the same within measurement accuracy. Also, one expects cathodes (1) and (2) to be similar though not to the extent as for cathodes (3) and (4). As the maximum QE is almost the same within measurement accuracy for the four cathodes, we have to analyze the Fourier coefficients A_0 to B_4 to find out whether the various cathodes are similar in layered structure and stoichiometry.

These Fourier coefficients are also shown in fig. 3 and it is immediately obvious from this figure that the coefficients evolve in a similar way for cathodes (1, 2) and (3, 4) respectively. To determine if different cathodes are formed for different Cs deposition rates, we consider the Fourier coefficients at the time of maximum QE (indicated by the vertical lines in fig. 3). The curves show that A_0 varies from 0.31 (1) to 0.37 (4), A_2 varies from 0.11 (4) to 0.23 (2), A_4 varies from -0.02 (1) to 0.07 (3,4) and finally B_4 varies from 0.13 (2) to 0.16 (4). This seems to indicate that

the various cathodes have different ellipsometric angles Ψ and Δ at the time of maximum QE. This means that the cathodes have a different layer structure and/or index of refraction. The latter would indicate a different stoichiometry for the cathodes.

This is further collaborated by the different shape of the curves for the Fourier coefficients for deposition times smaller than the time for maximum QE, especially between those for cathodes (1, 2) and (3, 4) respectively. This again illustrates that these cathodes have different thickness and/or refractive indices. This demonstrates that ellipsometry is capable of resolving different layer thickness and/or refractive index of the photocathode during the formation of the cathode. Especially the refractive index provides additional information about the composition of the layer, though additional characterization of Cs-Te with different stoichiometry is required to correlate the refractive index to a particular stoichiometry.

CONCLUSIONS

Although Cs-Te photocathodes have shown to have both a high quantum efficiency and long lifetime, and are therefore very suitable for use in photocathode RF accelerators for free-electron lasers, its lack of reproducibility is still an issue. To fully understand the underlying physics additional real-time diagnostics tools are required to monitor and probe the composition and structure of the photocathode during its formation. Ellipsometry, as a non-destructive, optical diagnostic tool for measuring the properties of thin films, seems an ideal candidate. Indeed, we have shown that a real-time, rotating compensator ellipsometer can be used to follow the formation of the cathode as it is grown in our preparation chamber. We were not able to derive the ellipsometric angles Ψ and Δ , and hence layer thickness and index of refraction, from these measurements as the unknown ellipsometric angles of the existing vacuum window of the preparation chamber do not allow calculation of these variables from the measured data. Still, this data showed that cathodes made with different Cs deposition rates have different ellipsometric data. Ellipsometry is therefore a very useful diagnostic tool that can be used to monitor index of refraction and thickness of the layers as the cathode is grown.

ACKNOWLEDGEMENT

This research is supported by the European Community, Research Infrastructure Activity under the FP6 "Structuring the European Research Area" program (CARE, Contract No. RII3-CT-2003-506395).

REFERENCES

- [1] V. Ayvazyan et al., *Eur. Phys. J. D* **37** 297 (2006).
- [2] S.H. Kong et al., *Nucl. Instrum. Methods Phys. Res. A* **358** 272 (1995).
- [3] P. Michelato *Nucl. Instrum. Methods Phys. Res. A* **393** 455 (1997).
- [4] I. Boscolo and P. Michelato, *Nucl. Instrum. Methods Phys. Res. A* **445** 389 (2000).
- [5] R.A. Loch, *Cesium-Telluride and Magnesium for high quality photocathodes*, Master Thesis, University of Twente (2005).
- [6] J. Teichert et al., Report on photocathodes, CARE/JRAPHIN (2004)
- [7] D. Sertore et al., *Nucl. Instrum. Methods Phys. Res. A* **445** 422 (2000).
- [8] P. Michelato et al., Proceedings EPAC96 1510 (1996)
- [9] D. Sertore et al., Proceedings EPAC06 2496 (2006).
- [10] A. Fry et al., Proceedings LINAC98 642 (1998).
- [11] S.H. Kong et al., *J. Appl. Phys.* **77** 6031 (1995).
- [12] S.H. Kong et al., *Nucl. Instrum. Methods Phys. Res. A* **358** 276 (1995).
- [13] D.C. Nguyen et al., *Nucl. Instrum. Methods Phys. Res. A* **429** 125 (1999).
- [14] S.H. Kong et al., *Nucl. Instrum. Methods Phys. Res. A* **358** 284 (1995).
- [15] J.W.J. Verschuur et al., *Nucl. Instrum. Methods Phys. Res. B* **139** 541 (1998).
- [16] B. van Oerle, *A High Brightness Electron Beam for Free Electron Lasers*, PhD Thesis, University of Twente (1997).
- [17] I.V. Volokhine, *Design and Numerical Analysis of TEU-FEL II*, PhD Thesis, University of Twente (2003).
- [18] A. di Bona et al., *J. Appl. Phys.* **80** 3024 (1996).
- [19] E. Chevallay et al., CERN CTF3 Note 020 (2001).
- [20] S. Valeri et al., *Thin Solid Films* **352** 114 (1999).
- [21] P. Michelato et al., *Nucl. Instrum. Methods Phys. Res. A* **393** 464 (1997).
- [22] A.H. Sommer. *Photoemissive materials. Preparation, Properties and Uses*, New York, John Wiley & Sons, Inc (1968).
- [23] R.A. Powell et al., *Phys. Rev. B* **8** 3987 (1973).
- [24] H. G. Tompkins, E. A. Irene (eds.), *Handbook of Ellipsometry* William Andrew, Inc., 2005
- [25] P.S. Hauge and D.H. Hill, *Opt. Comm.* **14** 431 (1975)